

## Proton-induced fission of $^{232}\text{Th}$ and Ir: Exciton model calculations

B. P. Pathak\* and L. Lessard

*Laboratoire de Physique Nucléaire, Université de Montréal, Montréal, Québec, Canada H3C 3J7*

(Received 31 January 1985)

Exciton model calculations within the geometry-dependent hybrid model have been performed to study the proton-induced fission of  $^{232}\text{Th}$  and Ir. After adjusting the parameters of the model to reproduce observed  $(p, xn)$  and total fission cross section, isotopic distributions of Rb and Cs have been evaluated and compared with experimental distributions measured by on-line mass spectrometry. With simplifying assumptions on the charge division mechanism, the experimental Cs distributions are very well reproduced in the  $^{232}\text{Th}(p, f)$  case. Observed structures are explained in terms of reaction mechanisms. The fission of medium-heavy elements [e.g.,  $\text{Ir}(p, f)$ ] appears to be promising for studying high excitation energy fission events and angular momentum effects.

### I. INTRODUCTION

The proton-induced fission of heavy and medium-heavy nuclei has been studied using a variety of methods ranging from radiochemical methods to solid state particle detectors. Excitation energies from a few MeV to those attained with beams of a few hundred MeV have been produced. The results obtained in these studies have been summarized by a number of reviewers.<sup>1-5</sup> During the last few years, on-line mass spectrometry<sup>6</sup> has enabled the measurement of independent yields of short lived species which are not accessible by radiochemical methods. The ion sources constructed for on-line mass spectrometers were limited first to the alkalis. Recent developments<sup>7</sup> have allowed the measurements of indium and gallium yields. It should be possible, with further improvements, to extend the technique to other elements (with negative ions, such as bromine,<sup>8</sup> or in oxide form, such as strontium<sup>9</sup>).

The fission yields measured by on-line mass spectrometry give the isotopic distribution for a given element. From this distribution, one can obtain the postneutron average mass of this particular element, the width, and the other moments.<sup>10</sup> From the centroid of the distribution one can, in certain instances, infer the total number of neutrons  $\nu_T$  corresponding to a given charge split. Indeed, for the actinides, it is fortunate that two alkalis ( $^{37}\text{Rb}$  and  $^{55}\text{Cs}$ ) are very nearly complementary, and that indium ( $Z=49$ ) is nearly the product of symmetric fission.

It is found that  $\nu_T$  increases with the energy of the incident projectile. This increase, which is approximately one neutron per 9 MeV at lower incident energies, slows down as the projectile energy increases.<sup>10,12,13</sup> This observation indicates that as the incident projectile energy increases, a larger fraction of the available energy is not used to evaporate neutrons.

Another conspicuous feature is the appearance of a well-defined structure of the Cs distributions at the higher mass side for larger incident energies.<sup>10-12</sup> This structure has been attributed to low excitation energy fission events with very few neutrons emitted prior to fission, since the

observed "bump" in the distribution is centered<sup>10</sup> at a value corresponding to the distribution measured with very low incident energy ( $< 30$  MeV). This asymmetry, which is clearly seen in the Cs distributions obtained with U and Th targets, is absent from the indium distributions.<sup>10-13</sup> This is in agreement with the published qualitative explanation, since indium is produced in nearly symmetric fission with possibly a higher fission barrier.<sup>14</sup>

All the observations indicate an increasingly important direct reaction contribution to fission with higher incident proton energies. It remains to give a quantitative theoretical evaluation of the processes involved.

Considerable progress has been made, within the so-called exciton model,<sup>15</sup> in explaining the interactions of energetic projectiles with various targets. In the course of a collision, a variety of processes take place: compound nucleus formation, particle transfers, excitation by multiple interaction, and preequilibrium particle emission. The relative amplitudes of these processes depend on the energy of the incident projectile, and also on the structures of the target and projectile. In the actinide region, where the fission barriers and neutron separation energies are comparable, one cannot attribute fission events following the irradiation of a target with energetic projectiles to a single excited nucleus of known  $A$  and  $Z$ . On the contrary, the observed fission cross section is the result of a sum of contributions from a number of excited nuclei with different atomic and mass numbers, and a wide spectrum of excitation energies. The success of the exciton model in reproducing a host of nuclear reactions<sup>16</sup> makes it an ideal candidate for unraveling the complex phenomena leading to fission.

In the present work, we have studied the proton-induced fission of medium-heavy ( $A \sim 190$ ) and actinide nuclei ( $A \sim 232$ ), where results of our calculations can be compared with our own experimental results. Competition between preequilibrium decay, particle emission, and fission has been evaluated within the geometry dependent hybrid model, which incorporates the exciton model and the master equation approach of Harp, Miller, and Berne. We have used the computer program ALICE (Ref. 17) to investigate the reaction mechanism within that model.

In the case of proton-induced fission of  $^{232}\text{Th}$ , a series of papers has been published by Hogan and co-workers<sup>18,19</sup> who have used the exciton model (the approach of Gadioli *et al.*<sup>20</sup>) to understand the data obtained by radiochemical methods. Considerable success was achieved in reproducing excitation functions [such as (p,xn), (p,pxn), etc.]. With a proper adjustment of a few parameters, the fission, preequilibrium, and evaporation contributions are well accounted for. To understand the observed behavior of the most probable charge ( $Z_p$ ), a distinction was made between symmetric and asymmetric fission mechanisms, and a relation was obtained for deciding by which mode a given nucleus would fission. It was found that, to reproduce observed  $Z_p$  values, UCD (unchanged charge distribution) and MPE (minimum potential energy) charge division postulates had to be adopted for symmetric and asymmetric fission modes, respectively.

Our objective partially overlaps with the program of Hogan and co-workers. We will use Blann's approach. (For our study, the differences between the approaches of Gadioli *et al.* and Blann are not significant since we are mainly concerned with cross section evaluations. With proper parameter adjustment, both methods yield equally good cross section values.) Our main concern, however, is in explaining the observed Rb and Cs isotopic distributions and understanding the origin of the previously mentioned structure in the Cs distributions. To do this, the energy dependence of the intrinsic width of the isotopic distributions had to be assumed, and various charge division hypotheses were studied.

In our calculations on the proton-induced fission of iridium, we have much less extensive data to make comparisons. On the other hand, a comparison between results of calculations shows that the medium-heavy region is probably a much better region for studying excitation energy effects on the fission mechanism, whereas the actinide region provides a very good test for studying the role of the reaction mechanism.

## II. THEORY

### A. General considerations

According to the exciton model,<sup>15</sup> the energy of the incident projectile is shared with the target nucleus through a number of successive binary interactions. In the course of this process, more and more complicated states are excited, but at each stage a fraction of states have particles that are unbound, and some of the nucleons may escape before complete equilibrium is reached. This phenomenon is known as preequilibrium (or precom-

pound) emission. The kinetic energies of the emitted particles prior to equilibrium are very widely distributed with a maximum close to the energy of the incident projectile.

In its early form, the exciton model was used for calculating relative spectral shapes. By combining this model with the master equation approach of Harp, Miller, and Berne,<sup>21</sup> it was possible to calculate angle integrated absolute cross sections. This modified version is known as the hybrid model.<sup>16</sup>

It was soon realized that major spectral contributions were produced at the nuclear surface. To take the nuclear surface into account, a geometry dependent nucleon density  $d(R)$  was included. A Fermi density distribution was assumed so that, at a radius  $R$ , one had

$$d(R) = \bar{d} [\exp(R - c)/(Z + 1)]^{-1}, \quad (1)$$

where  $c = 1.07A^{1/3}$  and  $Z = 0.55$  fm. The nucleon mean free path was also assumed to follow the same pattern.

The decays of equilibrated nuclei formed after precompound emission proceed by particle emission and fission (when energetically possible). The cross sections for particle evaporation are calculated in the computer program ALICE by using the Weisskopf-Ewing method.<sup>22</sup> The fission cross section at each stage is calculated by the Bohr-Wheeler approach using angular momentum dependent ground state and saddle point energies as given by the rotating liquid drop model (LDM).

### B. Adjustable parameters

The free parameters of the calculation are the level density parameter  $a$ , the ratio of the level density parameter appropriate to saddle point  $a_f$  and that appropriate to equilibrium deformation  $a_n$ , and the nucleon mean free path (MFP). The values of these parameters were fixed by fitting the experimentally measured spallation and fission cross sections.

For iridium, the level density parameter was taken to be  $A/12$ , as suggested by Døssing and Jensen.<sup>23</sup> The ratio  $a_f/a_n$  was taken to be 1.1 to fit the trend of fission cross sections measured by Stéphan<sup>24</sup> in this mass region. The mean free path obtained with the optical potential incorporated in the computer program ALICE,  $\lambda_{\text{NN}}$ , was used. The calculated LDM fission barrier for an iridium target (18.8 MeV) was found to be considerably lower than the experimental value (22.6 MeV).<sup>25</sup> In the present calculation, we used a multiplying factor of 1.17 which was found to yield values close to the experimental quantities in this mass region.

For thorium, the mean free path and the  $a_f/a_n$  ratio were adjusted to get good fits of the (p,xn), (p,pxn), and

TABLE I. Parameters used in the present calculations.

| Nucleus | Exciton number |         | $a$    | MFP                      | $\frac{a_f}{a_n}$ |
|---------|----------------|---------|--------|--------------------------|-------------------|
|         | Proton         | Neutron |        |                          |                   |
| Thorium | 1.2            | 0.8     | $A/8$  | $1.5\lambda_{\text{NN}}$ | 1.06              |
| Iridium | 1.2            | 0.8     | $A/12$ | $\lambda_{\text{NN}}$    | 1.1               |

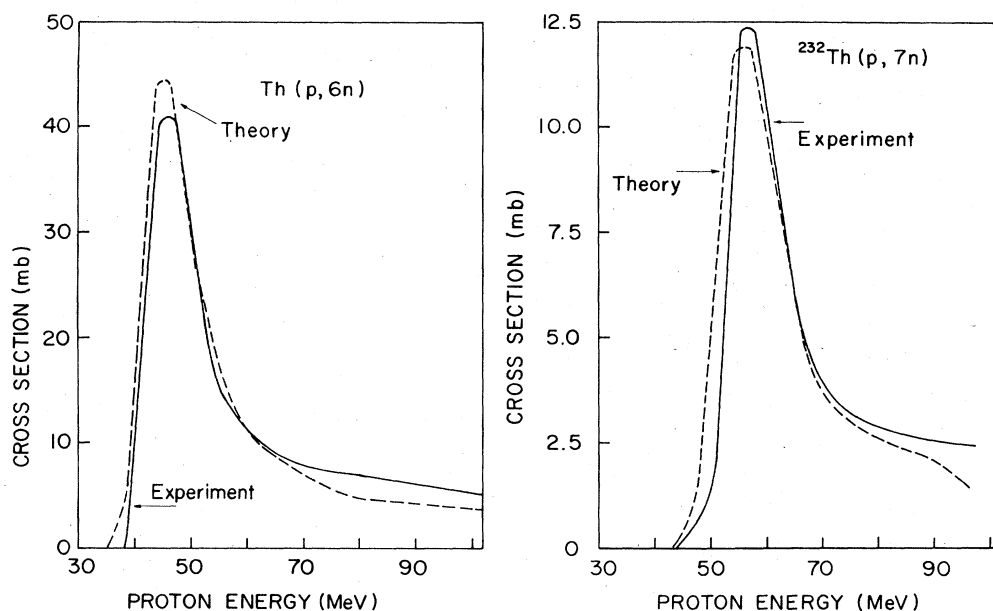


FIG. 1. Comparison of calculated (p,6n) and (p,7n) cross sections with the experimental values.

fission cross section data.<sup>26</sup> Figure 1 shows the quality of the agreement between our calculations and the (p,6n) and (p,7n) experimental cross sections. The value of the level density parameter was chosen to be  $A/8$ . A value of the mean free path of  $1.5\lambda_{NN}$  was necessary to obtain good agreement with measured (p,6n) and (p,7n) cross sections. In the latter case, the cross sections of Suk, Crawford, and Moore<sup>26</sup> were taken to be the most precise, among some divergent published values, as the counting techniques used by these authors were direct and subject to less uncertainty. With this choice of parameters, the (p,n), (p,2n), and (p,3n) cross sections reported by Kudo *et al.*<sup>14</sup> were found to be in excellent agreement with the calculated values. More recently published values of (p,xn) and (p,pxn) cross sections, measured by Hogan *et al.*,<sup>19</sup> were equally well reproduced. Table I gives a summary of the parameters used in the present calculations.

### III. RESULTS

In the present work, our interest has been to understand the isotopic distributions measured by on-line mass spectrometry. The most important quantities are the calculated cross sections for precompound emission and the quantitative evaluation of the competition between fission and particle evaporation from equilibrated excited nuclei. This competition, in turn, yields the relative magnitudes of the various multichance fission cross sections.

As the projectile energy increases, precompound emission becomes dominant, and the compound nucleus contribution diminishes. As a result, in the fission induced by protons of increasing energy, the fraction of the fissioning nuclei formed by precompound processes becomes more and more important. This makes the study of fission reactions at these energies correspondingly more complicated. Indeed, the nucleons resulting from precom-

pound emission have their energies almost uniformly distributed from a few MeV to very close to the energy of the incident protons (see Fig. 2). Consequently, the residual nuclei have excitation energies distributed over a broad spectrum. While analyzing fission data obtained with such a target-projectile system, this wide energy distribution must be taken into account.

In this work, the relative contributions to the fission cross section from nuclei of different excitation energies were calculated as follows: The cross section for compound nucleus formation  $\sigma_{CN}$  was calculated by the program ALICE; the energy spectra of the residual nuclei  $\sigma(E)$  following precompound emission were obtained from the

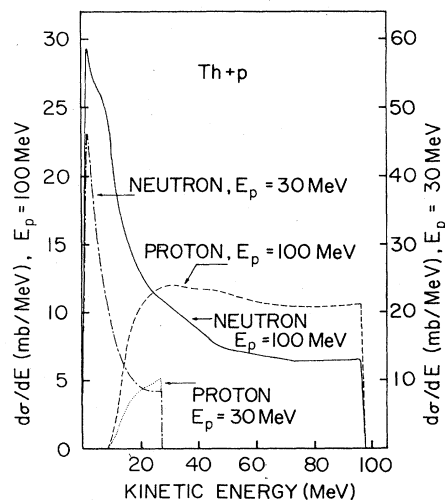


FIG. 2. Energy spectra of precompound neutrons and protons at 97 and 30 MeV incident proton energy on thorium target.

projectile energy and  $\sigma_p$ , the energy of the emitted nucleon (precompound nucleon), with the usual corrections for the nucleon binding energies. The binding energies of the neutrons and protons were obtained from Wapstra and Gove.<sup>27</sup>

The cross sections  $\sigma_{\text{CN}}$  and  $\sigma_p(E)$  thus obtained were then used to calculate multichance fission cross sections at each stage of the neutron evaporation chain. The fission to neutron emission rate  $\Gamma_f/\Gamma_n$  was calculated by using the simplified relation given by Vandenbosch and Huizenga:<sup>28</sup>

$$\frac{\Gamma_n}{\Gamma_f} = \frac{4A^{2/3}a_f(E - B_n)}{K_0 a_n [2a_f^{1/2}(E - E_f)^{1/2} - 1]} \times \exp[2a_n^{1/2}(E - B_n)^{1/2} - 2a_f^{1/2}(E - E_f)^{1/2}], \quad (2)$$

where the only not yet defined quantity is  $K_0$  ( $=\hbar^2/2mr_0^2$ ) with  $m$ , the neutron mass. Thus the fission cross section for a residual nucleus (formed either by precompound emission or neutron evaporation) is given by

$$\sigma_f = \sigma_R(E) \frac{\Gamma_f(E)}{\Gamma_f(E) + \Gamma_n(E)}. \quad (3)$$

The excitation energy of the fissioning nucleus at each stage of the multichance fission process was determined with the assumption that each evaporated neutron will produce a 9 MeV decrease of the excitation energy. The evaporation cross section for charged particles is small and was, therefore, neglected. In the calculation of  $\Gamma_f/\Gamma_n$ , the experimental values of  $E_f$  and  $B_n$  were used.

The excitation energies of the fission fragments ( $E_{f1}^* + E_{f2}^*$ ) were calculated by using the relation

$$E_{f1}^* + E_{f2}^* = E_{\text{c.m.}} - E_{k,\text{tot}} + Q_0, \quad (4)$$

where  $E_{\text{c.m.}}$  is the energy available in the entrance channel (in the center-of-mass system) after allowing for the emission of particles, as described above.  $E_{k,\text{tot}}$  is the kinetic energy of the fragments and  $Q_0$  is the energy released if the primary fragments are produced in their ground states. The values of  $E_{k,\text{tot}}$  were evaluated using the expression given by Viola,<sup>29</sup>

$$E_{k,\text{tot}} = 0.1071 \frac{Z^2}{A^{1/3}} + 22.2 \text{ (MeV)}. \quad (5)$$

Nuclear masses given by Wapstra and Gove<sup>27</sup> were used to calculate  $Q_0$ .

The numbers of neutrons emitted by the primary fragments were taken to be

$$\nu_{\text{post}} = \frac{E_{f1}^* + E_{f2}^*}{9}. \quad (6)$$

The numbers of pre-fission neutrons and the masses of fissioning nuclei are obtained from the relative contributions to the fission cross section from nuclei of different masses, as given by program ALICE. The total number of neutrons ( $\nu_{\text{post}} + \nu_{\text{pre}}$ ) can be directly compared with the

corresponding experimental quantities: e.g., for the proton induced of  $^{232}\text{Th}$ ,

$$\nu_T = 233 - \bar{A}_{\text{Rb}} - \frac{54}{55} \bar{A}_{\text{Cs}}, \quad (7)$$

$$\nu_T = 233 - \frac{36}{37} \bar{A}_{\text{Rb}} - \bar{A}_{\text{Cs}}. \quad (8)$$

Thus the total numbers of neutrons emitted can be evaluated from the measured centroids of the isotopic distributions of complementary (or near complementary) fragments as in the case of the Rb-Cs pair for the  $^{232}\text{Th}(p,f)$  reaction. Similar expressions exist for obtaining  $\nu_T$  from the centroids of the indium distributions [for  $^{232}\text{Th}(p,f)$ ; see Ref. 10] or from the centroids of the rubidium distributions [for Ir( $p,f$ ); see Ref. 30].

To calculate the isotopic distributions, two types of information are required, which are not included in exciton model calculations. The exciton model provides the nuclear reaction input (fissioning species, with its excitation energy, and formation cross section). Another essential input is a model for the charge separation between the fission fragments. Two competing prescriptions have been widely used: UCD (unchanged charge distribution) and ECD (equal charge displacement). Our analysis of the mass spectrometer measurements of the Rb-Cs isotopic distributions indicate that the charge division mechanism does not vary with the energy of the incident proton (in the 29–100 MeV range). For ease of calculation, we have chosen to replace ECD by an equivalent formulation given by Chatterjee<sup>31</sup> who proposed the equal sharing of excess neutrons. In this hypothesis it is assumed that the fragments are produced, for a given  $Z$ , in the stable configuration for that charge, and that the excess neutrons are shared equally between the two fragments. In the present work it was considered merely as a useful ansatz for calculation purposes.

The second piece of information needed to obtain isotopic distributions is the intrinsic width of the distribution for a given fissioning species leading to a certain fragment element. At lower energies, this width has been shown to be independent<sup>31</sup> of excitation energy. Throughout our calculations, we have assumed no energy dependence for this width. In the case of Rb-Cs, we have used the widths measured by Chaumont<sup>32</sup> for the isotopic distributions for those elements produced in the thermal neutron-induced fission of  $^{235}\text{U}$  (FWHM =  $3.60 \pm 0.07$  mass units).

The postneutron mass of fragments depends on the number of evaporated neutrons. A prescription is required to obtain the excitation energy sharing between the heavy and light fragments. Throughout the present work, we have assumed that

$$\frac{E_H^*}{E_L^*} = \frac{m_H}{m_L} \quad (9)$$

in obvious notation. This is slightly at variance with the usual assumption that  $\nu_H/\nu_L \sim 2$  for the Rb-Cs pair.<sup>10</sup> If our assumption is incorrect, the calculated centroids of the Rb and Cs distributions will deviate from the experimental values in a systematic way.

### A. The $^{232}\text{Th}(p,f)\text{Rb,Cs}$ reaction

In our previous experimental study of the  $^{232}\text{Th}(p,f)$  reaction, we measured isotopic distributions of Cs and Rb fission fragments at incident energies ranging from 29 to 97 MeV. The integrated Cs and Rb cross sections were found to evince little variation with incident energy, thus following the same trend as the total fission cross section over the same energy range. In other words, the fraction of the fission events leading to a Rb-Cs pair is approximately energy invariant. We have used this observation to infer the contributions of various fissioning species to the Rb and Cs distributions.

Program ALICE gives the cross sections for compound nucleus and precompound emission at 1 MeV energy intervals. We calculated the isotopic distributions of Rb and Cs from these data for each 1 MeV interval. The distributions assigned to compound nucleus and residues of precompound emission are shown in Fig. 3. In these calculations, we used the method just described. For a given excitation energy of a fission fragment, the number of neutrons evaporated from the fragment is obtained by assuming that each evaporated neutron takes away a fixed amount of excitation energy (assumed to be 9 MeV). Thus for a given excitation energy of the fissioning nucleus a certain fraction goes to each fragment [see Eq. (9)] which, in turn, evaporates some neutrons. In this way, one obtains an isotopic distribution which has to be folded with the intrinsic (low energy) width of the isotopic distributions. The calculation allows one to identify the various fissioning species responsible for different regions of the distributions. This is important if we want to understand the origin of the structure observed in the Cs distributions. These calculations have been reported with the

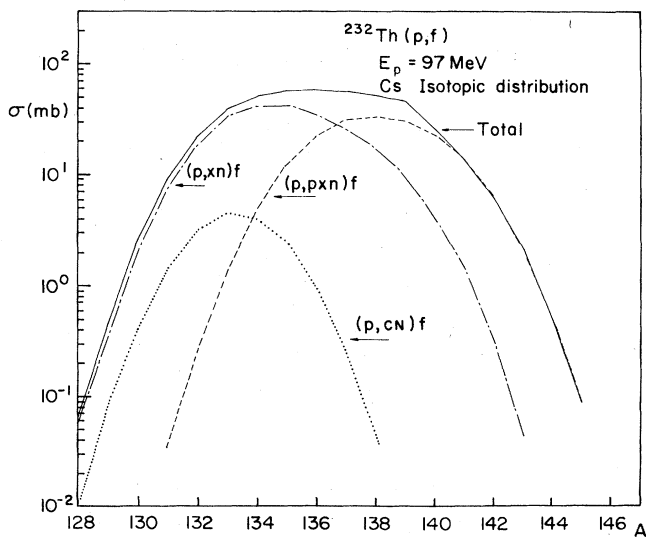


FIG. 3. Contributions of calculated  $(p,\text{CN})$ ,  $(p,xn)$ , and  $(p,pxn)$  reactions including precompound emission to Cs isotopic distribution for 100 MeV incident proton energy on thorium target. The values are not normalized to obtain experimental total cross sections.

two above-mentioned charge division postulates.

The results of calculations are shown in Figs. 4 and 5 for Rb and Cs. The overall agreement, with the ECD assumption, is remarkably good for Cs at all energies except for the 29 MeV case. The discrepancy in the latter case can be explained if one takes into account the experimental method used for making these measurements. The overall thickness of the target assembly system was such that the energy spread of the beam in the target was not negligible at 29 MeV. This would produce a lower effective mean energy, which would explain the mass shift of the theoretical curve with respect to the experimental data.

The asymmetric structure of the Cs distributions is clearly visible in Fig. 5. The origin of the structure can be easily understood by looking at Fig. 3 which shows the relative contributions to the isotopic distribution of the compound nucleus mechanism  $\sigma(p,f)$  and the two evaporation chains  $\sigma(p,xnf)$  and  $\sigma(p,pxnf)$ . Obviously, the heavy mass side is nearly totally due to the  $(p,pxnf)$  reaction. The evolution of the structure, which becomes more and more important as the energy increases, comes entirely from the  $(p,pxnf)$  behavior as a function of incident energy (see Fig. 6).

To understand the reason for the different contributions of the  $(p,xnf)$  and  $(p,pxnf)$  mechanisms, one must consider the energy spectra of the emitted neutrons and protons as calculated by program ALICE and shown in Fig. 2. The neutron spectrum contains a high percentage of low kinetic energy particles, which are due, to a large extent, to an evaporationlike mechanism. These low energy particles are therefore emitted by nearly equilibrated nuclei and correspond to higher excitation energy events. Because of the Coulomb barrier, these evaporation events are absent from the proton spectrum. Protons are emitted almost exclusively in precompound events, which means that the average excitation energy of the fissioning nucleus after proton emission is substantially lower than after neutron emission.

An alternate way of looking at the same phenomenon is to consider the excitation energy spectrum of the fissioning nuclei, as shown in Figs. 7 and 8. Again it is seen that the average excitation energy of the  $(p,pxn)$  events is much lower than for the  $(p,xn)$  events.

An interesting piece of information can be obtained from this separation between  $(p,xnf)$  and  $(p,pxnf)$  events. Obviously, the simple extraction of  $\nu_T$  using expressions (7) and (8) cannot be used at higher incident proton energies, since no provision is made in these expressions for proton emission. On the other hand, if one uses the centroids from the  $(p,xnf)$  calculations, one can obtain directly the number of neutrons values associated with these events. This is what we attempted to do in our previous paper<sup>10</sup> by subtracting the heavy mass side contribution from the Rb-Cs distributions. The  $\nu_T$  values thus obtained compared very well with the quantities extracted from the In distributions. This result is consistent with the observations that the indium distributions show no heavy mass structure and are substantially narrower than the Cs distributions. It is readily explained if one accepts the results of Kudo *et al.*<sup>14</sup> which indicate a higher fis-

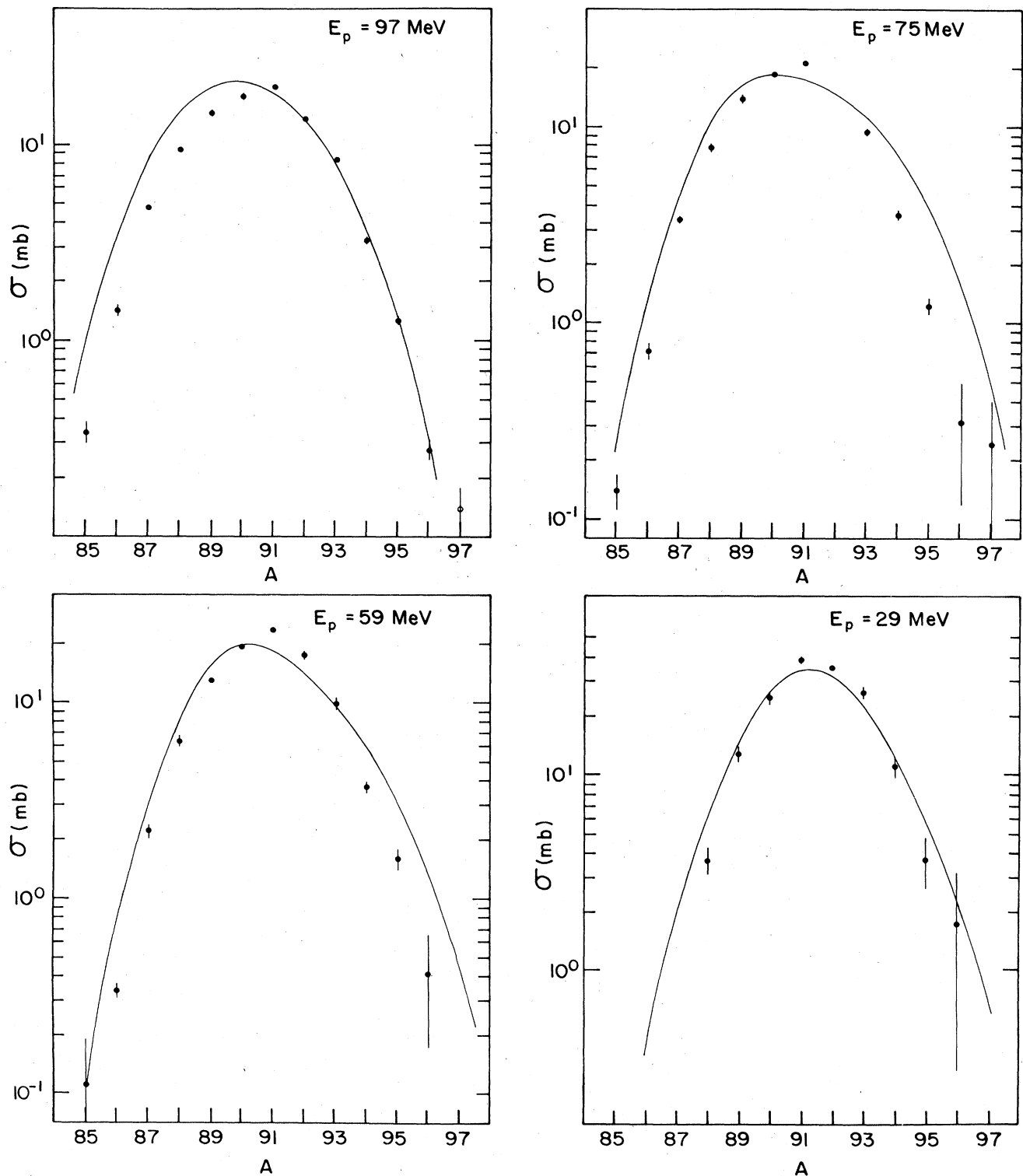


FIG. 4. Calculated and measured isotopic distributions of Rb from proton-induced fission of thorium.

fusion barrier ( $\sim 9 \text{ MeV}$ ) for symmetric fission, as compared to asymmetric fission ( $\sim 6 \text{ MeV}$ ). This higher barrier would suppress very effectively the lower excitation energy events produced in  $(p,pxn_f)$  reactions. Figure 9

shows the  $\nu_T$  values calculated for the  $(p,pxn_f)$  as compared to the quantities obtained from the In and Rb-Cs distributions.

A more quantitative way of comparing our calculations

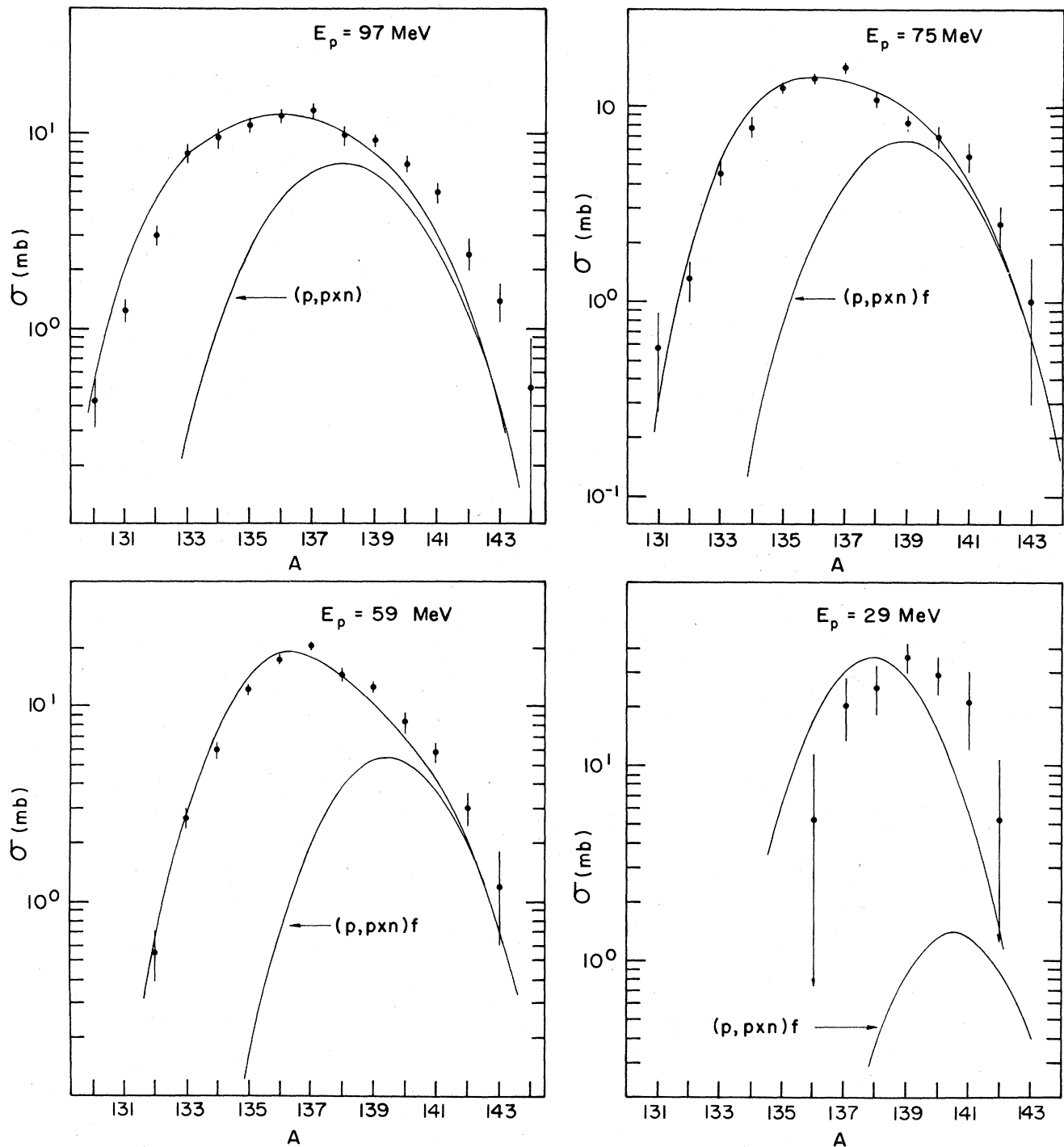


FIG. 5. Calculated and measured isotopic distributions of Cs from proton-induced fission of thorium. The calculated  $(p,pxn)f$  contribution is explicitly shown.

with the observed shapes is to compare the moments of the calculated and experimental distributions. This is done in Tables II and III. The centroids of the distributions are related to the numbers of neutrons emitted in the total fission process (prior to fission and postfission). The

agreement is very good (assuming ECD) both for Rb and Cs. Since conclusions are usually drawn on the fission mechanism by taking into account only the centroid values, one might conclude that the above-mentioned agreement is strong evidence in favor of ECD. On the

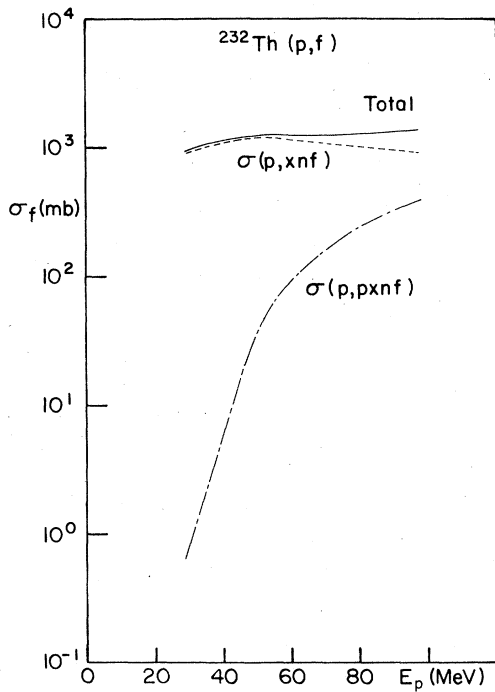


FIG. 6. Variation of contribution to total fission cross section from precompound emission residues in the  $^{232}\text{Th}(p,f)$  reaction.

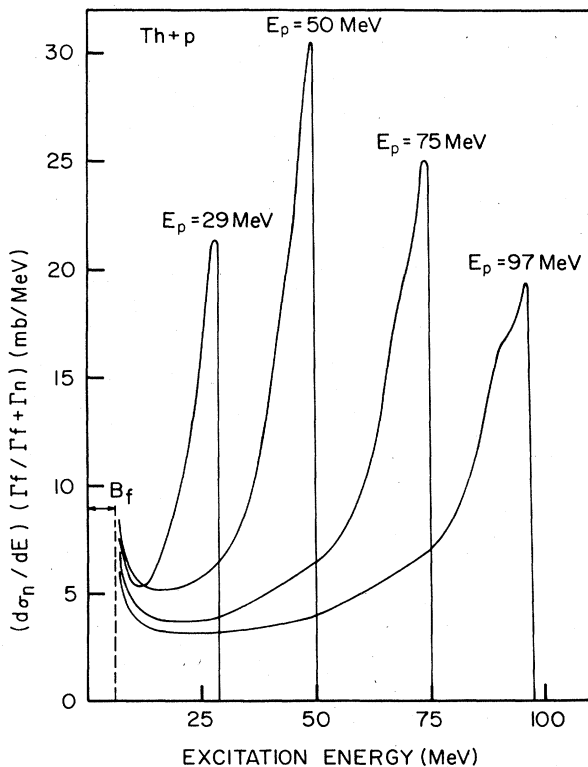


FIG. 7. Energy spectra of fissioning nuclei after precompound neutron emission for proton-induced fission of thorium.

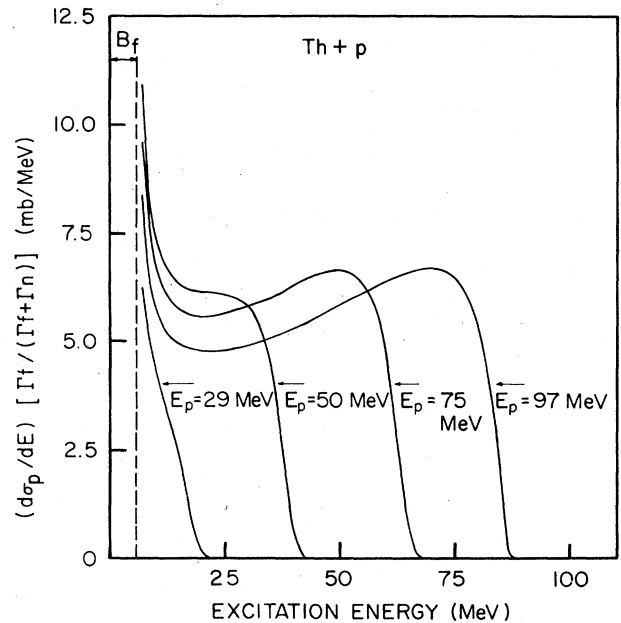


FIG. 8. Energy spectra of fissioning nuclei after precompound proton emission for proton-induced fission of thorium.

other hand, the evidence from the other moments is far from being as conclusive. The shape of the Cs distributions appears to be equally well reproduced with either assumption, whereas the Rb shapes seem to be better accounted for with the UCD hypothesis. We believe, however, that this comparison should not be pressed too hard to extract definite information on the charge division mechanism since the exact shapes of the distributions do depend on the reaction mechanism. Suffice it to say that the reaction cross sections evaluated with the exciton model yield good representations of the observed isotopic distributions with centroids shifted more or less depending on the charge division hypothesis used. ECD appears to produce the right shift.

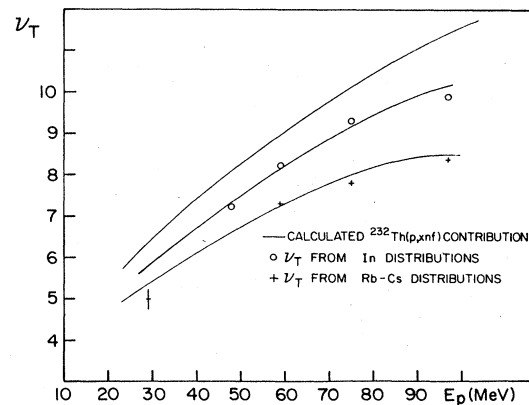


FIG. 9.  $\nu_T$  (total number of neutrons emitted per fission event) obtained from Rb-Cs distributions and indium distributions in the  $^{232}\text{Th}(p,f)$  reaction. Calculated  $\nu_T$  for  $(p,pxnf)$  reaction is shown for comparison.



TABLE II. Moments of Rb isotopic distribution in  $^{232}\text{Th}(p,f)\text{Rb}$ .

| $E_p$<br>(MeV) | Centroid<br>(u) |       | Variance<br>( $u^2$ ) |      |        |       | Skewness |       |        |        | Excess |        |
|----------------|-----------------|-------|-----------------------|------|--------|-------|----------|-------|--------|--------|--------|--------|
|                | Theory          |       | Theory                |      | Theory |       | Theory   |       | Theory |        | Theory |        |
|                | UCD             | ECD   | UCD                   | ECD  | UCD    | ECD   | UCD      | ECD   | UCD    | ECD    | UCD    | ECD    |
| 95             | 91.21           | 89.98 | 4.29                  | 4.35 | 3.80   | 0.70  | 0.105    | 0.022 | -0.214 | -0.216 | -0.054 | -0.054 |
| 75             | 91.58           | 90.72 | 3.94                  | 5.06 | 3.45   | 0.178 | 0.303    | 0.077 | -0.189 | -0.322 | 0.073  | 0.073  |
| 59             | 91.86           | 90.86 | 3.36                  | 4.34 | 3.06   | 0.200 | 0.452    | 0.069 | -0.063 | -0.059 | 0.071  | 0.071  |
| 29             | 92.50           | 91.58 | 2.43                  | 3.94 | 2.69   | 0.056 | 0.294    | 0.080 | 0.042  | -0.326 | 0.070  | 0.070  |

TABLE III. Moments of Cs isotopic distribution in  $^{232}\text{Th}(p,f)\text{Cs}$ .

| $E_p$<br>(MeV) | Centroid<br>(u) |        | Variance<br>( $u^2$ ) |      |        |       | Skewness |       |        |        | Excess |       |
|----------------|-----------------|--------|-----------------------|------|--------|-------|----------|-------|--------|--------|--------|-------|
|                | Theory          |        | Theory                |      | Theory |       | Theory   |       | Theory |        | Theory |       |
|                | UCD             | ECD    | UCD                   | ECD  | UCD    | ECD   | UCD      | ECD   | UCD    | ECD    | UCD    | ECD   |
| 97             | 135.62          | 136.20 | 6.51                  | 7.05 | 7.78   | 0.147 | 0.130    | 0.18  | -0.431 | -0.484 | -0.32  | -0.32 |
| 75             | 136.27          | 136.79 | 5.52                  | 5.88 | 6.35   | 0.294 | 0.315    | 0.22  | -0.326 | -0.400 | -0.27  | -0.27 |
| 59             | 136.61          | 137.12 | 4.36                  | 4.76 | 4.97   | 0.415 | 0.455    | 0.28  | -0.069 | -0.116 | -0.19  | -0.19 |
| 29             | 137.60          | 138.01 | 2.46                  | 2.59 | 2.16   | 0.070 | 0.181    | 0.235 | -0.089 | 0.235  | 0.235  | 0.235 |

### B. The Ir(p,f)Rb reaction

Because of the higher fission barrier of iridium the Ir(p,f)Rb reaction is very different from the  $^{232}\text{Th}(p,f)$  reaction. Although the total reaction mechanism is nearly as complex, the fraction of the reaction products leading to fission is much smaller for iridium than for thorium. Our previous experimental measurements<sup>30</sup> have produced relative cross section measurements of the Rb isotopes at three proton energies (62, 80, and 95 MeV) on natural iridium. From these data, information was extracted on the number of emitted neutrons. The purpose of the present calculations is to understand the reaction mechanism leading to fission in the iridium region and throw some light on the role this type of reaction can play in the study of high excitation energy fission.

The total fission cross sections for iridium, as calculated by ALICE, are in very good agreement with the trend of the measured total Rb fission cross sections, as shown in Fig. 10, which indicates that our choice of parameters is satisfactory. Although our measurements have been done at energies where the precompound emission dominates, thus producing residual excited nuclei at energies ranging from zero to the maximum value allowed by the incident projectile energy (see Fig. 11), it is easily seen that only a narrow range of excitation energies lead to fission events. When weighed with  $\Gamma_f/(\Gamma_n + \Gamma_f)$ , this distribution shows a sharp peak with a width of about 10 MeV and an average excitation energy near the compound system value (see Fig. 12). Thus, fission in this mass region, for the incident energies used in our experiment, can be attributed to compound nucleus or quasicompound nucleus decay. Also a significant, although not very large, contribution to the total fission cross section is due to events following proton emission.

Contrary to the case of  $^{232}\text{Th}(p,f)$ , very few nuclear species participate to fission following proton bombardment of iridium, which means that fission occurs more rapidly in the evaporation chain. These calculations yield readily the average number of neutrons (and protons) emitted prior to fission.

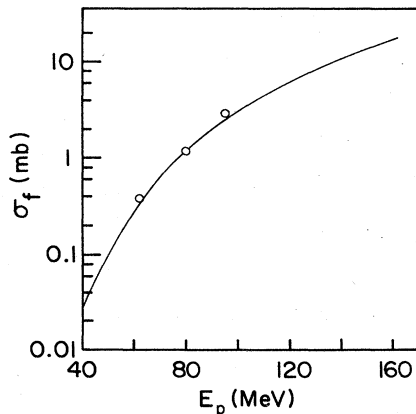


FIG. 10. Calculated (continuous line) and measured (circles) variation of relative fission cross section of iridium with incident proton energy.

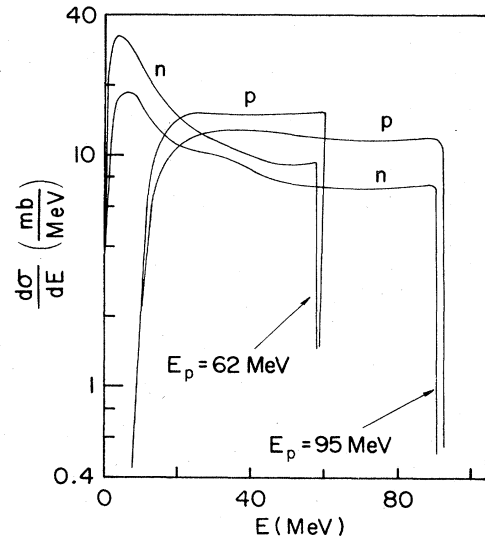


FIG. 11. Energy spectra of neutrons and protons emitted in the proton bombardment of an iridium target.

From the calculated excitation energy of the fission fragment, and assuming that the fission process can be described by the UCD hypothesis (which holds for symmetric fission), one obtains

$$\bar{A}_{\text{Rb}} = 37 \frac{A_f}{Z_f} - \frac{E^*}{9} \quad (10)$$

The isotopic distribution was calculated in the manner described above. A good agreement with the measured distributions, i.e., a symmetric shape with a width of 3.5 mass units, is obtained also in good agreement with the experimentally observed values. The results are summarized in Table IV.

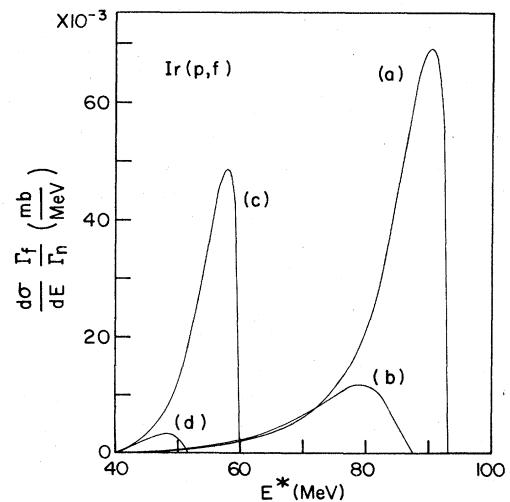


FIG. 12. Relative contribution to fission cross section from nuclei formed after precompound emission. The curves *a* and *b* are for residues of neutrons and protons, respectively, at 95 MeV incident energy. The curves *c* and *d* represent the contributions from neutron and proton emission residues, respectively, at 62 MeV proton energy.

TABLE IV. Calculated average mass  $\langle a_f \rangle$  and charge  $\langle Z_f \rangle$  of fissioning nuclei produced in the proton-induced fission of  $^{193}\text{Ir}$  and deduced postfission and prefission neutrons.

| Incident<br>proton<br>energy<br>(MeV) | $\langle A_f \rangle$ | $\langle Z_f \rangle$ | $\langle \nu_{pre} \rangle$ | Measured<br>$\langle A \rangle_{\text{Rb}}$ | $\frac{\langle A \rangle_{\text{Sym.}}}{\langle A \rangle_{\text{Rb}} \times Z_f}$<br>= $\frac{\langle A \rangle_{\text{Sym.}}}{37 \times 2}$ | $\langle A \rangle_{\text{Sym.}}$<br>Corrected for<br>$^{193}\text{Ir}$ admixture | $\langle \nu_{post} \rangle$ | $\langle \nu_T \rangle$ |
|---------------------------------------|-----------------------|-----------------------|-----------------------------|---------------------------------------------|-----------------------------------------------------------------------------------------------------------------------------------------------|-----------------------------------------------------------------------------------|------------------------------|-------------------------|
| 62                                    | 191.49                | 78.00                 | 0.51                        | 88.13                                       | 92.96                                                                                                                                         | 92.57                                                                             | 6.35                         | 6.86                    |
| 80                                    | 191.06                | 77.99                 | 0.94                        | 87.72                                       | 92.45                                                                                                                                         | 92.06                                                                             | 6.94                         | 7.88                    |
| 95                                    | 190.79                | 77.98                 | 1.21                        | 87.37                                       | 92.07                                                                                                                                         | 91.69                                                                             | 7.42                         | 8.63                    |

It is interesting to note that the  $\nu_T$  values obtained by using the simplified assumption that all the fission cross section was due to compound nucleus and those obtained by using the calculated average energy, mass, and charge are in excellent agreement. This result is indicative of the fact that the most significant contribution to fission comes from the highest permissible excitation energies.

The calculations yield the number of prefission neutrons which, although small, is not negligible. The calculated isotopic distribution depends on the total excitation energy of the system leading to fission, and not on the details of when the neutrons are evaporated (whether it is before fission occurs or from the excited fission fragments). This is due to the fact that the excitation energy carried away by an emitted neutron is rather insensitive to the mass of the emitting nucleus.

#### IV. CONCLUSION

In the course of these calculations based on the exciton model (geometry dependent hybrid model), it is found that by using reasonable values of a few parameters, it is possible to reproduce and explain a wide range of experimental data. In particular, the mean free path and level density parameters can be chosen so as to give very good agreement with the observed  $(p, xn)$ ,  $(p, pxn)$ , and fission reaction cross sections. This having been achieved, the essential characteristics of fission are reasonably well reproduced. Besides providing a relatively simple model to understand the fission phenomena in the actinide and iridium mass regions, these calculations reveal a number of interesting features.

Firstly, the fact that in the medium-heavy nuclei the only significant contribution comes from a narrow distribution of excited nuclei gives us an opportunity to investigate fission phenomena at high excitation energies without noticeable interference from nuclei of low excitation energies formed in the reaction. In particular, it is possible to study angular momentum effects in the fission process by comparing proton- and heavy-ion-induced fission in nuclei of comparable masses and excitation energies.<sup>30,33</sup>

Secondly, the asymmetry observed in the distributions of the Cs isotopes in the proton-induced fission of  $^{232}\text{Th}$  is explained in terms of the energy and mass distributions of the nuclei formed in the reaction process. The amount of asymmetry may be useful in understanding the relative strengths of different processes leading to the formation of fissionable nuclei. To achieve this, precise knowledge

of the intrinsic (i.e., low energy) isotopic distributions is required. The study of the proton-induced fission of the actinides by the on-line mass spectrometer technique at low incident energies (10–20 MeV) will provide useful data for this purpose.

Another point of interest is the success of the extremely simple assumption of equal sharing of excess neutrons (double center model of Chatterjee) in reproducing the experimental results. It has been shown by Chatterjee that the DCM model very nearly approximates the ECD hypothesis. The results of our calculations appear to substantiate the conclusions of our experimental study of the  $^{232}\text{Th}(p, f)$  reaction, namely, that the ECD postulate is valid for asymmetric fission, even at high excitation energies.

In the course of this work, several simplifying assumptions were made, and some effects have been neglected. It remains to analyze the implications of these simplifications.

One important assumption has been to use identical cross sections for the production of Cs and Rb at all energies. This is nearly true if one considers the total Cs (or Rb) cross sections which are measured to be 93, 93, 104, 114, and 143 mb at incident proton energies of 97, 75, 59, 50, and 29 MeV, respectively. On the other hand, since the asymmetric contribution to fission decreases with increasing excitation energy (from 100% to about 50% in the energy range of interest), this result implies an increasing contribution of the symmetric mode to the Cs cross section with increasing proton energy.

Had we taken into account the interplay of symmetric and asymmetric fission modes, we would have had to consider possible differences in the fission barriers for the two modes. The net result would have been to enhance the relative importance of the heavier isotopes in the isotopic distributions, since they are produced at lower excitation energies, where asymmetric fission is favored. It would be possible then to obtain better agreement with the measured heavy side of the distributions, but this agreement would be somewhat artificial, since there is no *a priori* method of deciding on the importance of either mode.

The effect of  $\gamma$  emission accompanied by neutron evaporation has also been neglected in the present calculation. The average energy loss by  $\gamma$  emission per fission event (per neutron emitted for  $^{236}\text{U}$ ) has been estimated by Nifenecker *et al.*<sup>34</sup> to be about 1.1 MeV. This would also have the effect of shifting the isotopic distributions towards the heavy side. In the present work, no attempt was made to include corrections for  $\gamma$  emission as it is be-

lied that the uncertainty caused by other factors may be larger than the one due to the energy loss by this process.

Another simplification is the assumption that the intrinsic widths of the distributions are independent of excitation energy. Although verified up to  $\sim 40$  MeV excitation energy,<sup>35</sup> this assumption may not be valid at higher energies. However, the expected variation should not be so important as to modify the predicted isotopic distributions. The shapes of these distributions are mainly determined by the reaction mechanism and charge division

postulated.

To summarize, the present simplified approach explains all the essential features of the isotopic distributions of Rb and Cs produced in the proton-induced fission of  $^{232}\text{Th}$ . Some understanding of the different characteristics of the indium distributions is also obtained. Better quantitative agreement could be reached by making further assumptions, but our understanding of the phenomenon would not be substantially improved.

- 
- \*Present address: Canadian Centre for Occupational Health and Safety, Hamilton, Ontario, Canada.
- <sup>1</sup>H. A. Nifenecker, J. Blachot, J. P. Bocquet, R. Brissot, J. Crançon, C. Hamelin, G. Mariolopoulos, and C. Ristori, in *Proceedings of the International Symposium on Physics and Chemistry of Fission, Jülich, 1979* (International Atomic Energy Agency, Vienna, 1980), p. 35.
  - <sup>2</sup>I. S. Grant, *Rep. Prog. Phys.* **39**, 955 (1976).
  - <sup>3</sup>H. J. Specht, *Rev. Mod. Phys.* **46**, 778 (1974).
  - <sup>4</sup>D. C. Hoffman and M. M. Hoffman, *Annu. Rev. Nucl. Sci.* **22**, 65 (1972).
  - <sup>5</sup>M. Brack, J. Damgaard, A. S. Jensen, H. C. Pauli, V. M. Strutinsky, and C. Y. Wong, *Rev. Mod. Phys.* **44**, 320 (1972).
  - <sup>6</sup>R. Klapisch, J. Chaumont, C. Philippe, I. Amarel, R. Fergeau, M. Salomé, and R. Bernas, *Nucl. Instrum. Methods* **53**, 216 (1967).
  - <sup>7</sup>L. Nikkinen, B. P. Pathak, L. Lessard, and J. K. Lee, *Nucl. Instrum. Methods* **175**, 425 (1980).
  - <sup>8</sup>Blake Sutherland, M.S. thesis, McGill University, 1977.
  - <sup>9</sup>P. L. Reeder, L. J. Alquist, J. Lin, and J. F. Wright, *Nucl. Instrum. Methods* **133**, 501 (1976).
  - <sup>10</sup>L. Nikkinen, B. P. Pathak, L. Lessard, and I. S. Grant, *Phys. Rev. C* **22**, 617 (1980).
  - <sup>11</sup>B. L. Tracy, J. Chaumont, R. Klapisch, J. M. Nitschke, A. M. Poskanzer, E. Roeckl, and C. Thibault, *Phys. Rev. C* **5**, 222 (1972).
  - <sup>12</sup>J. K. P. Lee, G. Pilar, B. L. Tracy, and L. Yaffe, *J. Inorg. Nucl. Chem.* **37**, 2035 (1975).
  - <sup>13</sup>K. C. Chan, B. P. Pathak, L. Nikkinen, L. Lessard, and I. S. Grant, *J. Inorg. Nucl. Chem.* **39**, 1915 (1977).
  - <sup>14</sup>H. Kudo, H. Muramatsu, H. Nakahara, K. Miyano, and I. Kohno, *Phys. Rev. C* **25**, 3011 (1982).
  - <sup>15</sup>J. J. Griffin, *Phys. Rev. Lett.* **17**, 478 (1966).
  - <sup>16</sup>M. Blann, *Annu. Rev. Nucl. Sci.* **25**, 123 (1975).
  - <sup>17</sup>M. Blann, University of Rochester Report No. COO-3494-29, 1976.
  - <sup>18</sup>Chien Chung and James Hogan, *Phys. Rev. C* **24**, 180 (1981).
  - <sup>19</sup>J. Hogan, E. Gadioli, E. Gadioli-Erba, and C. Chung, *Phys. Rev. C* **20**, 1831 (1979).
  - <sup>20</sup>E. Gadioli, E. Gadioli-Erba, and J. J. Hogan, *Phys. Rev. C* **16**, 1404 (1977).
  - <sup>21</sup>G. D. Harp, J. M. Miller, and B. J. Berne, *Phys. Rev.* **165**, 1166 (1968).
  - <sup>22</sup>V. F. Weisskopf and D. H. Ewing, *Phys. Rev.* **57**, 472 (1940).
  - <sup>23</sup>T. Døssing and A. S. Jensen, *Nucl. Phys.* **A222**, 493 (1974).
  - <sup>24</sup>Claude Stéphane, Ph.D. thesis, Faculté des Sciences, Orsay, 1965.
  - <sup>25</sup>P. A. Seeger and W. M. Howard, *Nucl. Phys.* **238**, 491 (1975).
  - <sup>26</sup>H. C. Suk, J. E. Crawford, and R. B. Moore, *Nucl. Phys.* **A218**, 418 (1974).
  - <sup>27</sup>A. H. Wapstra and N. B. Gove, *Nucl. Data Tables* **A9**, 267 (1971).
  - <sup>28</sup>R. Vandenbosch and J. R. Huizenga, *Nuclear Fission* (Academic, New York, 1973), p. 233.
  - <sup>29</sup>V. E. Viola, Jr., *Nucl. Data* **1**, 391 (1966).
  - <sup>30</sup>B. P. Pathak, L. Lessard, L. Nikkinen, and J. K. Lee, *Phys. Rev. C* **25**, 2534 (1982).
  - <sup>31</sup>M. L. Chatterjee, *Phys. Lett.* **66B**, 319 (1977).
  - <sup>32</sup>J. Chaumont, Ph.D. thesis, Faculté des Sciences, Orsay, 1970.
  - <sup>33</sup>W. Reisdorf, M. de Saint-Simon, L. Lessard, L. Remsberg, C. Thibault, E. Roeckl, R. Klapisch, I. V. Kuznetsov, Yu. Ts. Oganessian, and Yu. E. Penionshkevitch, *Phys. Lett.* **62B**, 33 (1976).
  - <sup>34</sup>H. Nifenecker, C. Signarbieux, R. Babinet, and J. Poitou, in *Proceedings of the International Symposium on Physics and Chemistry of Fission, Jülich, 1974* (International Atomic Energy Agency, Vienna, 1974), p. 117.
  - <sup>35</sup>J. A. McHugh and M. C. Michel, *Phys. Rev.* **172**, 1160 (1968).